A biomechanical study to optimize superior capsular reconstruction operative technique

Suhas P. Dasari, MD[a], Amar S. Vadhera, BS[b], Mariano E. Menendez, MD[c], Zeeshan A. Khan, BA[d], Nozomu Inoue, PhD[d], Elizabeth Shewman, MS[d], Brian R. Waterman, MD[e], Grant E. Garrigues, MD[d], Brian J. Cole, MD MBA[d], Nikhil N. Verma, MD[d,*]

[a]Department of Orthopaedics and Sports Medicine, University of Washington, Seattle, WA, USA
[b]Sidney Kimmel Medical College, Philadelphia, PA, USA
[c]Oregon Shoulder Institute, Medford, OR, USA
[d]Division of Sports Medicine, Midwest Orthopaedics at Rush, Department of Orthopaedic Surgery, Rush University Medical Center, Chicago, IL USA
[e]Atrium Health Wake Forest Baptist, Wake Forest University School of Medicine, Winston-Salem, NC, USA

Background: The goals of this study were to optimize superior capsular reconstruction by assessing the relative fixation strength of 4 suture anchors; evaluating 3 glenoid neck locations for fixation strength and bone mineral density (BMD); determining if there is a correlation between BMD and fixation strength; and determining which portal sites have optimal access to the posterosuperior and anterosuperior glenoid neck for anchor placement.

Methods: Twenty cadaveric specimens were randomized into 4 groups: all-suture anchor (FiberTak), conventional 3.0-mm knotless suture anchor (SutureTak), 3.9-mm knotless PEEK (polyetheretherketone) Corkscrew anchor, and 4.5-mm Bio-Corkscrew anchor. Each specimen was prepared with 3 anchors into the glenoid: an anterosuperior anchor, superior anchor, and posterosuperior anchor. All anchors were inserted into the superior glenoid neck 5 mm from the glenoid rim. A materials testing system performed cyclic testing (250 cycles) followed by load-to-failure testing at 12.5 mm/s. Cyclic elongation, first cycle excursion, maximum load, and stiffness were recorded. Using custom software, BMD was calculated at each anchor location. This software was also used to assess access to the posterosuperior and anterosuperior glenoid neck from standard arthroscopic portal positions.

Results: There was no significant difference in cyclic elongation ($P = .546$), first cycle excursion ($P = .476$), maximum load ($P = .817$), or stiffness ($P = .309$) among glenoid anchor positions. Cyclic elongation was significantly longer in the PEEK Corkscrew group relative to the other implants ($P \leq .002$). First cycle excursion was significantly greater in the FiberTak group relative to all other implants ($P \leq .008$). For load-to-failure testing, the Bio-Corkscrew group achieved the highest maximum load ($P \leq .001$). No other differences in cyclic or failure testing were observed between the groups. No differences in stiffness testing were observed ($P = .133$). The superior glenoid rim had the greatest BMD ($P = .003$), but there was no correlation between BMD and cyclic/load outcomes. The posterior portal (80% of specimens) and the anterior portal (60% of specimens) demonstrated the best access to the posterosuperior and anterosuperior glenoid neck, respectively.

Conclusion: The 4.5-mm Bio-Corkscrew anchor provided the most robust fixation to the glenoid during superior capsular reconstruction as it demonstrated the strongest maximum load, had minimal elongation, had minimal first cycle excursion, and did not fail during cyclic testing. The superior glenoid neck had the highest BMD; however, there was no correlation between BMD or glenoid anchor location and biomechanical outcomes. The posterior portal and anterior portal provided optimal access to the posterosuperior glenoid neck and anterosuperior glenoid neck, respectively.

Superior capsular reconstruction (SCR) is a relatively new surgical intervention that was developed for the management of symptomatic, irreparable rotator cuff tears in younger patients with minimal glenohumeral osteoarthritis.[17] Within the glenohumeral joint, the superior capsule functions as a static stabilizer to block superior translation of the humeral head and also provides dynamic reinforcement to the rotator cuff itself.[14] In the setting of irreparable rotator cuff tears, SCR rebalances coupling forces between the rotator cuff structures in order to simultaneously improve the compression and depressor effects of the rotator cuff and joint capsule leading to enhanced stability.[14] Additionally, the graft also functions as a soft-tissue spacer and links the anterior and posterior rotator cuff.[30] This leads to a significant clinical improvement in biomechanical function and pain at the glenohumeral joint.[17,31]

Biomechanically, cadaveric studies have largely demonstrated positive results with SCR.[31] The procedure leads to a significant decrease in the superior translation of the humeral head and in subacromial contact pressures.[14] This biomechanical benefit of SCR has translated to the clinical setting with generally positive results.[6,9,19,20]

While SCR has demonstrated good results, it is a relatively new technique that requires further refinement for the optimization of clinical and biomechanical outcomes. During SCR, the dermal graft is typically fixed to the native anatomic attachments of the superior capsule.[2] Attachment points include the superior glenoid neck medially, the greater tuberosity laterally, and the remaining rotator cuff posteriorly.[2] While there is abundant literature evaluating suture anchor strength at the greater tuberosity (in the setting of rotator cuff repair) and at the glenoid chondrolabral junction (in the setting of labral repair), there is a paucity of data examining soft tissue to bone fixation at the glenoid neck.[8,10,12,15,21,23] Additionally, there exists disagreement regarding the optimal portal for placement of the posterosuperior glenoid anchor.[30]

Thus, the primary goals of this study were to further optimize the SCR technique by: (1) assessing the fixation strength of 4 different suture anchors to determine the optimum mode of fixation at the glenoid neck; (2) evaluating 3 locations: the anterosuperior, superior, and posterosuperior glenoid neck for anchor fixation strength and bone mineral density (BMD); (3) determining if there is a correlation between BMD and fixation strength; and (4) determining which portal sites have optimal access to the posterosuperior and anterosuperior glenoid neck for anchor placement.

Methods

This was an institutional review board exempt biomechanical study performed in a controlled laboratory setting with a total of 20 fresh-frozen deidentified cadaveric shoulders. The cadaveric specimens had no prior history of trauma or surgery to the shoulder joint, no history of cancer or related treatments, no history of chronic diseases that caused the patient to be bedridden, and no history of osteoporosis. Prior to dissection and testing, every specimen underwent a computed tomography (CT) scan (BrightSpeed, GE Medical Systems, Fairfield, CT, USA) to calculate the BMD (HU) and identify sites with maximal BMD for anchor fixation. Using 3D reconstructed models in Mimics Medical Software V24.0 (Materialise, Leuven, Belgium) and custom software, the BMD 5 mm medial to the chondrolabral junction at the 12 o'clock, 2 o'clock, and 10 o'clock positions were calculated for the corresponding superior, anterosuperior, and posterosuperior anchor positions, respectively. This was calculated to a depth of 15.0 mm which corresponded with the depth of the anchors used for this study.[4] Next, the accessibility of the posterosuperior and anterosuperior glenoid neck anchor position from the skin portal positions was determined (Fig. 1). A normal vector was projected from the target anchor position on the glenoid neck. Deviation from this orthogonal vector was calculated based on portal location on the specimen's skin. A deviation between 0° and 15° was considered minimal and allowed for good access for anchor placement. A deviation of 15°-30° was considered moderate and allowed for adequate access for anchor placement, a deviation of 30°-45° was considered severe with poor access for anchor placement, and a deviation greater than 45° was considered unacceptable due to its limited access to the glenoid neck for anchor placement. This model accounted for osseous obstruction from the acromion and coracoid process. For posterosuperior glenoid neck access, standard arthroscopic portals assessed included the portal of Wilmington, the posterolateral portal, and the posterior portal. For access to the anterosuperior glenoid neck, the anterior and anterolateral portals were assessed.

Specimens were then thawed at room temperature and mounted in the beach chair position from the medial scapular border. The sternoclavicular joint was rigidly stabilized through traction suspension, and a radiolucent bolt was utilized across the coracoclavicular interval to maintain a rigid construct in the native anatomic shoulder position. Specimens were placed into 1 of 4 groups: all-suture anchor (FiberTak; Arthrex, Naples, FL, USA), conventional 3.0-mm knotless suture anchor (SutureTak, Arthrex, Naples, FL, USA), 3.9-mm knotless PEEK (polyetheretherketone) Corkscrew anchor (Arthrex, Naples, FL, USA), and 4.5-mm Bio-Corkscrew anchor (Arthrex, Naples, FL, USA). After arthroscopic evaluation and débridement of the glenoid neck with an arthroscopic shaver or radiofrequency device, accessibility for anchor placement was assessed. Each scapula was prepared with 3 anchors into the superior glenoid: (1) an anterosuperior anchor at 2/10 o'clock (right/left), (2) a posterosuperior anchor at 10/2 o'clock (right/left), and (3) a superior anchor at 12 o'clock. All anchors were placed into the superior glenoid neck, 5 mm off of the glenoid rim, at the site of maximal bone density based on computed tomography measurements. All anchors were inserted according to the manufacturer's instructions.

Each scapula was then potted within a PVC (polyvinyl chloride) cylinder using acrylic cement (Isocryl; Lang Dental, Wheeling, IL, USA) and mounted at 30° of eversion in a custom fixture secured to the base of an electromechanical materials testing system (Insight 5; MTS, Eden Prairie, MN, USA). The free ends of the suture were attached to a custom jig in line with the load cell and tested in the following manner: (1) preload at 10 N for 2 minutes; (2) cyclic testing from 10 N to 60 N at 0.5 Hz for 250 cycles; and (3) load to failure at 12.5 mm/s. Time, load, and actuator displacement were synchronously recorded at 48 Hz using the MTS software (Testworks 4; MTS, Eden Prairie, MN, USA). For the cyclic testing, outcome measures included the total number of cycles that the construct completed, first cycle excursion, and cyclic elongation. First cycle excursion evaluates initial stability of the construct and is defined as the displacement of the crosshead from the start of testing to the peak of the first cycle. Cyclic elongation is defined as the distance the crosshead moved from the peak of cycle 1 to the peak of cycle 250. For the load-to-failure test, maximum load and mode of failure (anchor pullout, anchor-suture interface, suture, locking mechanism, bone fracture, or other) were determined. Stiffness was calculated as the steepest slope spanning 30% of the data points from initial to maximum load during the failure test.[24,26]
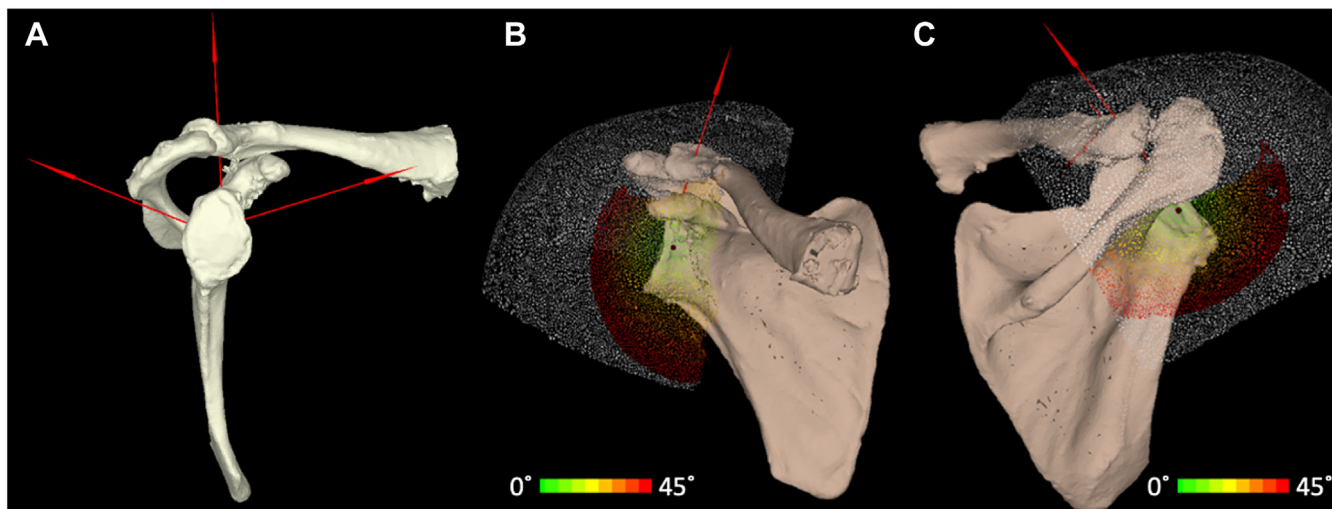
Figure 1 Three-dimensional (3D) reconstruction of a cadaveric right scapula demonstrating the normal vectors at the posterosuperior, superior, and anterosuperior glenoid neck positions (**A**). (**B** and **C**) Panels represent the relative deviation from a normal vector from the cortical surface. This normal vector is considered the optimal fixation angle for anchor placement. The deviation from this ideal angle is calculated based on skin portal placement when attempting to place anchors at the anterosuperior (**B**) and posterosuperior locations (**C**). For these representations, *green* indicates minimal deviation from this optimal angle while *red* indicates severe deviation from this optimal angle.

Statistical analysis

Data are presented as mean ± standard deviation unless otherwise stated. An a priori power analysis based on data using a similar methodology performed in our laboratory indicated that, for a statistical power of 80% with significance set at 0.05 and an effect size of 0.3, 10 specimens per group were required to detect differences in maximum load (10% difference). Normality of the data was confirmed using the Shapiro-Wilk normality test. A multi-way ANOVA (analysis of variance) was used to compare the effect of the anchor type and insertion location. If a significant difference was determined, a Bonferroni multiple-comparison test for multiple groups was used. A one-way ANOVA was used to compare BMD for the 3 anchor locations. A Pearson correlation test was used to quantify the relationship between outcome variables and BMD. A Kruskal-Wallis test was performed to compare BMD among the various anchor types as these measurements did not have a normal distribution. For this study, alpha was set at 0.05. All statistical analyses were performed utilizing software R (version 4.1.0; R Foundation for Statistical Computing, Vienna, Austria).

Results

Demographic characteristics

Twenty total specimens were included in this study; however, one specimen was excluded from biomechanical testing due to suspected poor bone quality. This specimen was still included in evaluation of access based on arthroscopic portal location. Due to the loss of this specimen in biomechanical testing, there were a total of 15 Bio-Corkscrew devices tested (5 specimens; n = 5 for the anterior, posterior, and superior locations), 14 FiberTak devices tested (5 specimens; n = 4 for the anterior location and n = 5 for the posterior and superior locations), 14 PEEK Corkscrew devices tested (5 specimens; n = 4 for the superior location and n = 5 for the anterior and posterior locations), and 14 SutureTak devices tested (5 specimens; n = 4 for the anterior location and n = 5 for the superior and posterior locations) that underwent cyclic testing. The average age of the specimens was 54.0 years (range: 20-63 years). There were 12 male and 8 female specimens. With regard to

laterality, there were 11 right-arm specimens and 9 left-arm specimens used in the study. The baseline BMD of the specimens was 276.1 ± 209.1 HU. There was no difference in average BMD among the FiberTak, knotless PEEK corkscrew, and Bio-Corkscrew anchor groups ($P = .075$). However, the average BMD of the SutureTak group was significantly higher than the other groups ($P = .030$).

Biomechanical outcomes

Cyclic testing

During cyclic testing, 2 SutureTak anchors in the anterosuperior position failed (cycles 83 and 106), one FiberTak anchor in the anterosuperior position failed (cycle 1), one FiberTak anchor in the superior position failed (cycle 9), one FiberTak in the posterosuperior position failed (cycle 11), and one PEEK Corkscrew in the anterosuperior position failed (cycle 0). The 3 FiberTak and 2 SutureTak devices failed via anchor pullout. For the single PEEK Corkscrew anchor, the device itself failed during device implantation. The pooled cyclic elongation and first cycle excursion measured from all specimens that completed cyclic testing were 6.72 ± 8.50 mm and 3.97 ± 2.21 mm, respectively (Table I).

Among the anchors that completed cyclic testing, there was no significant difference in cyclic elongation ($P = .546$) or first cycle excursion ($P = .476$) among the anterosuperior, superior, and posterosuperior glenoid neck anchor positions (Table II). However, there were significant differences between suture anchor groups during cyclic testing. Cyclic elongation was significantly larger in the PEEK Corkscrew group (15.31 ± 11.06 mm) than in all other suture-anchor groups (Table III, $P \leq .002$; Fig. 2). When examining first cycle excursion, the FiberTak group exhibited significantly longer excursion (6.29 ± 4.19 mm) than any other suture-anchor group (Table III, $P \leq .008$; Fig. 3). No other differences in first cycle excursion were noted among the remaining 3 anchor types. A summary of biomechanical outcomes stratified by anchor type and location is presented in Table IV.

Failure testing

Among the anchors that completed cyclic testing, pull to failure testing was then performed. The average overall failure to

Table I
Pooled biomechanical outcomes.

	Cyclic elongation (mm)	First cycle excursion (mm)	Maximum load (N)	Stiffness (N/mm)
Pooled value	6.72 ± 8.50	3.97 ± 2.21	200.25 ± 49.23	62.28 ± 8.63

N, Newton.

Table II
Comparison of biomechanical outcomes between positions.

	Anterosuperior	Posterosuperior	Superior	*P* value
Cyclic elongation (mm)	7.46 ± 8.96	5.72 ± 6.36	7.23 ± 10.45	.546
First cycle excursion (mm)	4.53 ± 3.46	3.96 ± 1.94	3.54 ± 0.79	.476
Maximum load (N)	202.69 ± 42.59	194.59 ± 54.93	205.6 ± 49.93	.817
Stiffness (N/mm)	61.34 ± 5.12	64.56 ± 10.33	60.51 ± 8.75	.309

N, Newton.

Table III
Comparison of biomechanical outcomes between suture-anchor groups.

	Bio-corkscrew	FiberTak	PEEK corkscrew	SutureTak	*P* value	Significant pairwise comparisons
Cyclic elongation (mm)	1.53 ± 0.78	5.25 ± 3.77	15.31 ± 11.06	3.08 ± 1.85	***P* < .001**	Bio-Corkscrew vs. PEEK Corkscrew: *P* < .001 Fibertak vs. PEEK Corkscrew: *P* = .002 PEEK Corkscrew vs. SutureTak: *P* < .001
First cycle excursion (mm)	3.39 ± 0.68	6.29 ± 4.19	3.62 ± 0.61	3.07 ± 0.44	***P* < .001**	Bio-Corkscrew vs. FiberTak: *P* = .004 FiberTak vs. PEEK Corkscrew: *P* = .008 FiberTak vs. SutureTak: *P* = .003
Maximum load (N)	253.56 ± 22.83	170.15 ± 47.74	178.81 ± 37.66	182.57 ± 32.30	***P* < .001**	Bio-Corkscrew vs. FiberTak: *P* < .001 Bio-Corkscrew vs. PEEK Corkscrew: *P* < .001 Bio-Corkscrew vs. SutureTak: *P* = .001
Stiffness (N/mm)	61.55 ± 4.29	62.15 ± 4.26	59.51 ± 14.03	67.65 ± 2.69	*P* = *.133*	N/A

N, Newton; *N/A*, not applicable.
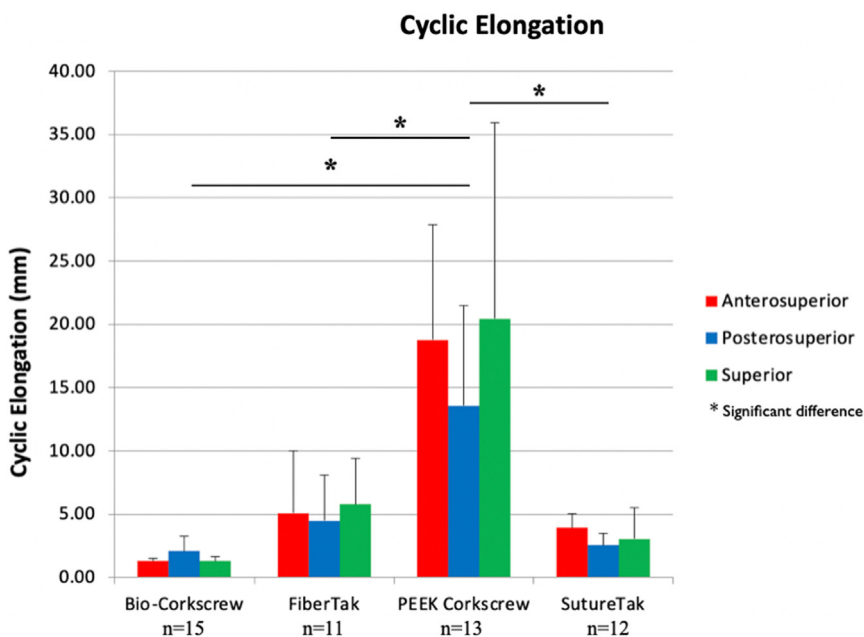Bold represents a significant difference.

Figure 2 Bar graph representing cyclic elongation for anchors that completed cyclic testing. There was no significant difference in cyclic elongation noted among anchor locations; however, the PEEK corkscrew group had significantly greater cyclic elongation than the other 3 anchors. No other statistically significant differences were noted.

load among all included specimens was 200.25 ± 49.23 N (Table I). When examining anchor location, there were no significant differences in maximum load among the anterosuperior, superior, and posterosuperior glenoid anchor positions (Table II, $P = .817$). When examining anchor types, the Bio-Corkscrew group achieved the highest maximum load (253.56 ± 22.83 N, Table III, $P \leq .001$; Fig. 4). No other differences in maximum load were observed among the groups. A summary of biomechanical
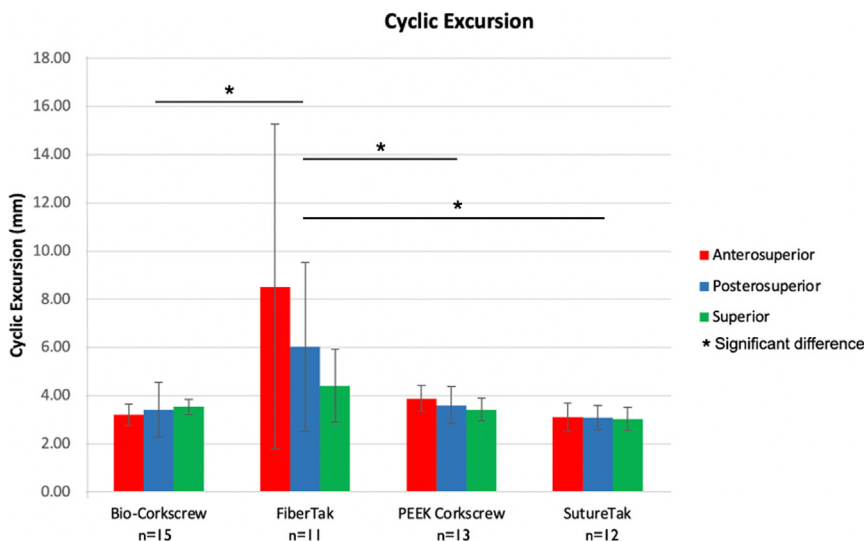
Figure 3 Bar graph representing first cycle excursion for anchors that completed cyclic testing. There was no significant difference in first cycle excursion noted among anchor locations; however, the FiberTak group had significantly greater first cycle excursion than the other 3 anchors. No other statistically significant differences were noted.

Table IV
A summary of biomechanical outcomes by anchor type and anchor position.

	Bio-corkscrew	FiberTak	PEEK corkscrew	SutureTak	P value (anchor subgroup analysis by location)
Cyclic Elongation (mm)	A: 1.27 ± 0.23 P: 2.05 ± 1.22 S: 1.29 ± 0.32	A: 5.09 ± 4.90 P: 4.47 ± 3.58 S: 5.75 ± 3.64	A: 18.8 ± 9.12 P: 11.7 ± 8.34 S: 16.8 ± 15.6	A: 3.91 ± 1.13 P: 2.51 ± 1.09 S: 3.22 ± 2.79	Bio-Corkscrew: .21 FiberTak: .82 PEEK Corkscrew: .61 SutureTak: .72
Cyclic Excursion (mm)	A: 3.21 ± 0.44 P: 3.42 ± 1.12 S: 3.53 ± 0.32	A: 8.52 ± 6.74 P: 6.03 ± 3.50 S: 7.55 ± 6.40	A: 3.88 ± 0.54 P: 3.60 ± 0.76 S: 3.42 ± 0.47	A: 3.10 ± 0.58 P: 3.09 ± 0.50 S: 3.03 ± 0.48	Bio-Corkscrew: .77 FiberTak: .54 PEEK Corkscrew: .56 SutureTak: .98
Maximum Load (N)	A: 238 ± 22.0 P: 262 ± 12.0 S: 260 ± 27.7	A: 206 ± 52.8 P: 144 ± 43.7 S: 149 ± 48.7	A: 166 ± 32.2 P: 191 ± 45.9 S: 175 ± 33.9	A: 182 ± 11.4 P: 167 ± 22.6 S: 199 ± 43.3	Bio-Corkscrew: .20 FiberTak: .26 PEEK Corkscrew: .60 SutureTak: .41
Stiffness (N/mm)	A: 62.2 ± 4.57 P: 61.8 ± 6.20 S: 60.7 ± 1.89	A: 64.0 ± 3.58 P: 62.1 ± 5.27 S: 60.3 ± 4.11	A: 55.9 ± 3.38 P: 66.3 ± 17.6 S: 54.3 ± 13.3	A: 66.2 ± 2.47 P: 68.0 ± 1.49 S: 68.1 ± 3.95	Bio-Corkscrew: .88 FiberTak: .62 PEEK Corkscrew: .33 SutureTak: .73

A, anterosuperior; *P*, posterosuperior; *S*, superior; *N*, Newton.

outcomes stratified by anchor type and location is presented in Table IV.

During testing, the reason for failure was recorded (Table V). For the 15 Bio-Corkscrew implants tested, the device failed at the anchor-suture interface (anchor failure) in 10 cases and failed at the suture in 5 cases. For the 14 FiberTak implants, 12 failed by anchor pullout, one failed at the suture material, and one classified as other. For the 14 PEEK Corkscrew implants, 9 failed at the locking mechanism, 2 pulled out, one anchor failed, and 2 fractured the bone. For the 14 SutureTak implants, 4 failed from anchor pullout, 7 failed at the anchor-suture interface (anchor failure), and 3 failed at the locking mechanism.

Stiffness testing

Among the anchors that completed cyclic testing, stiffness testing was performed. The average overall stiffness was 62.28 ± 8.63 N/mm (Table I). When examining stiffness by anchor location, there was no significant difference amongst the 3 anchor locations (Table II, $P = .309$). When examining anchor types, there was no significant difference in stiffness among the 4 tested anchors (Table III; $P = .133$).

Bone mineral density

BMD (HU) was evaluated at the anterosuperior, superior, and posterosuperior locations (Table VI). The mean BMD for the anterosuperior anchor location was 241.44 ± 165.70 HU. The mean BMD for the superior anchor location was 350.28 ± 254.28 HU. The mean BMD for the posterosuperior anchor location was 236.62 ± 187.71 HU. There was a significant difference in BMD among the 3 groups ($P = .003$) with the superior anchor location having a higher BMD than the anterosuperior ($P = .010$) and posterosuperior ($P = .007$) locations. There was no significant difference in BMD between the anterosuperior and posterosuperior locations ($P = .999$). Despite this, there was no correlation between BMD and maximum load ($P = .458$), cyclic elongation ($P = .408$), or first cycle excursion ($P = .498$) (Table VII).

Portal access

Using 3D reconstructed models in Mimics Medical Software V24.0 and custom software, access to the anterosuperior and posterosuperior glenoid neck from the skin was assessed
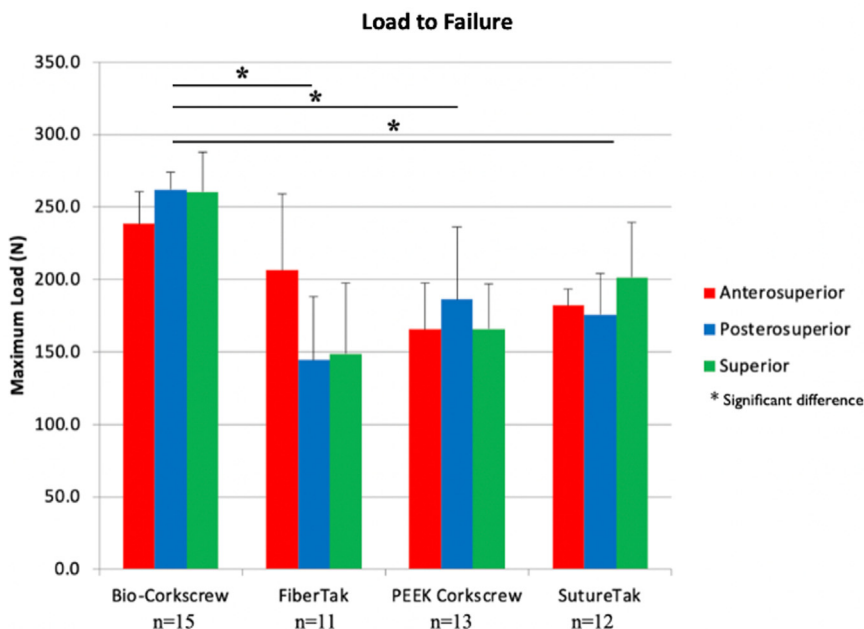
Figure 4 Bar graph representing load to failure for anchors that completed cyclic testing. There was no significant difference in load to failure noted among anchor locations; however, the Bio-Corkscrew group resulted in a significantly greater maximum load than the other 3 anchors. No other statistically significant differences were noted.

Table V
Mode of failure.

Device	Anchor pullout	Anchor failure	Suture failure	Locking mechanism	Bone fracture	Other
Bio-Corkscrew (n = 15)	0	10	5	0	0	0
FiberTak (n = 14)	12	0	1	0	0	1
Peek Corkscrew (n = 14)	2	1	0	9	2	0
SutureTak (n = 14)	4	7	0	3	0	0

Table VI
Comparison of glenoid densities between positions.

	Anterosuperior	Posterosuperior	Superior	P value
Density (HU)	241.4 ± 165.7	236.6 ± 187.7	350.3 ± 254.3	$P = .003$ Anterosuperior−posterosuperior: $P = .999$ Anterosuperior−superior: $P = .010$ Posterosuperior−superior: $P = .007$

HU, Hounsfield Units.
Bold represents a significant difference.

([Table VIII](#)). For the posterosuperior glenoid neck, the posterior portal had the highest frequency of acceptable access (80% of specimens). The posterolateral portal had the second highest frequency of acceptable access to the posterosuperior glenoid neck (50% of specimens), and the portal of Wilmington had the lowest frequency of acceptable access to the posterosuperior glenoid neck (15% of specimens). When examining access to the anterosuperior glenoid neck, the anterior portal was more likely to have acceptable access to this anchor location (60% of specimens) than the anterolateral portal location (25% of specimens).

Discussion

In this controlled laboratory investigation of the SCR procedure, cyclic elongation, first cycle excursion, maximum load, stiffness, and mode of failure were the primary outcomes tested at the anterosuperior, superior, and posterosuperior glenoid neck using 4 different anchor constructs. Notably, the Bio-Corkscrew was the only implant that had no instances of failure during cyclic testing. One PEEK, 3 FiberTak, and 2 SutureTak devices failed during cyclic testing. When examining the anchor devices, the PEEK corkscrew demonstrated the greatest cyclic elongation, while the FiberTak group demonstrated the greatest first cycle excursion. There were no other differences noted during cyclic testing. When subjecting the 4 anchor groups to load-to-failure testing, the Bio-Corkscrew group resulted in the greatest maximum load. There were no differences noted among the remaining 3 groups during load to failure testing. Additionally, when examining the primary outcomes based on anchor location, no difference was noted among the anterosuperior, superior, or posterosuperior anchor locations for cyclic elongation, first cycle excursion, or load to failure. The superior glenoid neck had a greater BMD than the posterosuperior and anterosuperior locations; however, there was no correlation between BMD and cyclic testing outcomes or load to failure outcomes. Among the standard arthroscopic portal positions examined, the posterior portal had the best access to the posterosuperior glenoid

Table VII
Pearson regression model for bone mineral density and biomechanical outcomes.

Variable	Correlation coefficient	95% confidence interval	P value
Density–maximum load	−0.15	−0.50 to 0.24	.458
Density–cyclic elongation	0.17	−0.23 to 0.51	.408
Density–first cycle excursion	0.14	−0.26 to 0.49	.498

Table VIII
Qualitative summary of portal access to posterosuperior and anterosuperior glenoid neck.

Portal location	Good access	Acceptable access	Poor access	Limited access	% acceptable access (n)
Posterosuperior anchor access					
Posterior portal	11	5	2	2	80% (16)
Posterolateral portal	5	5	7	3	50% (10)
Portal of Wilmington	1	2	5	12	15% (3)
Anterosuperior anchor access					
Anterior portal	6	6	6	2	60% (12)
Anterolateral portal	2	3	9	6	25% (5)

neck, while the anterior portal had the best access to the anterosuperior glenoid neck.

During biomechanical testing of the 4 anchors, the PEEK device and the FiberTak device performed poorest on cyclic testing, while the Bio-Corkscrew performed superior to all other devices during load-to-failure testing. There were no other significant differences noted. The PEEK device typically failed via its locking mechanism, and it is possible that its poor performance during cyclic testing with excessive cyclic elongation was due to this functional weakness in the construct. The FiberTak device demonstrated the greatest first cycle excursion, which may be attributable to knot slippage. Of note, there were no instances of failure during cyclic testing of the Bio-Corkscrew, while every other included device had at least one failure during cyclic testing. Taken together, these results would suggest that the 4.5-mm Bio-Corkscrew anchor provided the most robust fixation to the glenoid neck during SCR as it demonstrated the largest maximum load, had minimal elongation and first cycle excursion during cyclic testing, and did not fail during cyclic testing.

Fully threaded corkscrew anchors were developed to create maximal cortical purchase, and as a result, it is not surprising that the Bio-Corkscrew device had superior biomechanical testing relative to the SutureTak and FiberTak devices.[5] These all suture anchors have demonstrated inferior fixation, increased laxity, and increased displacement in bovine and cadaveric specimens.[7] Contrarily, it is surprising that the Bio-Corkscrew, which is composed of 15% beta-tricalcium phosphate and 85% poly-L-lactic acid, had superior load to failure testing results relative to the biostable PEEK Corkscrew device. The typical benefit of a biocompatible device is improved osteointegration and osteoconductivity, which would not be relevant in this ex vivo study design.[5] Instead, it is more likely that this is due to the size of the anchor utilized as the 4.5-mm Bio-Corkscrew had greater cortical bone purchase than the 3.9 mm PEEK Corkscrew anchor. Thus, in the context of prior biomechanical literature, this investigation would suggest that the 4.5-mm Bio-Corkscrew anchor provided the most optimal fixation of the graft at the glenoid neck during SCR procedures.

A second aim of this study was to explore anchor fixation strength at 3 superior capsule fixation locations on the glenoid neck. During cyclic testing, the anterosuperior position had 4 anchors that failed, while the superior and posterosuperior positions each had one anchor that failed. Additionally, there was no significant difference in load to failure, stiffness, cyclic elongation, or first cycle excursion at the anterosuperior, superior, or posterosuperior locations along the glenoid neck. This is of clinical significance as there is some controversy on the location of anchor placement for the medial fixation of the graft. The original technique by Mihata et al utilized 2 suture anchors to fix the graft at the glenoid neck at the superior and posterosuperior locations, while other authors propose variations in this technique with 3 anchors or anchors in the anterosuperior and posterosuperior locations.[2,13,16,22,25] The results of this study demonstrated no significant difference in anchor strength at the anterosuperior, superior, or posterosuperior locations, suggesting that any 2 of the 3 positions can provide

effective fixation during SCR. This would indicate that selection of anchor location is based on surgeon preference and factors such as access to the glenoid neck may be more important when selecting where to place the glenoid anchors.

This study also noted that the superior glenoid neck had a higher BMD than the other 2 glenoid positions tested; however, there was no correlation between BMD and cyclic elongation, first cycle excursion, or load-to-failure outcomes. This is reflected in the finding that the superior, anterosuperior, and posterosuperior glenoid neck location performed comparably on cyclic testing and load-to-failure testing despite calculated differences in BMD. Interestingly, prior investigations that sought to examine the relationship between fixation strength and BMD at other locations in the glenohumeral joint have demonstrated a significant relationship between the two. For example, two separate studies by Tingart et al demonstrated a significant, positive correlation between BMD and pullout strength for anchors placed at the tuberosities of the humerus.[28,29] Investigations at the chondrolabral junction have demonstrated similar findings with a positive correlation between BMD and anchor pullout strength.[18] Unlike the prior 3 studies, our investigation demonstrated no difference in cyclic or load to failure testing based on anchor location. When examining the mechanism of failure, the majority of implants failed extra-cortically (at the anchor-suture interface, the locking mechanism, or the suture itself). This may suggest that the BMD and corresponding fixation at the superior glenoid neck is stronger than the device itself leading to failure of the device during testing. This would potentially explain why there was no significant correlational relationship between BMD/anchor location and cyclic testing or load-to-failure testing outcomes.

In this study, the standard posterior portal and anterior portal provided the best access to the posterosuperior glenoid neck and anterosuperior glenoid neck, respectively, for optimal anchor placement. This is consistent with prior technical notes by the senior author, where standard anterior and posterior working portals were used to secure medial row fixation while using a standard lateral viewing portal.[3,11] Alternatively, if placing an anchor at the superior glenoid neck in the 12 o'clock position, adequate access can instead be achieved using the Neviaser portal.[2,30] This is of clinical significance as portal placement can dictate the angle of anchor fixation and subsequent construct strength. A biomechanical study by Strauss et al demonstrated that optimal soft tissue anchor fixation at the humerus occurred when the anchor was inserted orthogonal to the cortical surface.[27] Thus, when attempting to optimize fixation strength of the medial row during SCR, selecting portals that minimize deviation from this ideal anchor insertion angle will allow for maximal fixation strength.

Despite the promising results of this investigation, this study design had several limitations. As a biomechanical investigation performed in a controlled laboratory setting, this study is inherently limited in its applicability to the clinical setting. Results from an ex vivo cadaveric study may not accurately reflect the in vivo system, particularly when considering differences in bone quality between live patients and deceased cadaveric specimens.[1] Furthermore, as an ex vivo study, biological tissue healing and incorporation was not accounted for when testing the various implants.[1] An additional limitation of this investigation is that the cadaveric specimens were derived from predominantly older populations, while SCR is primarily indicated for younger, more active patient populations. Thus, the applicability of the findings from this investigation may be limited when repeated on cadaveric specimens that are more representative of the patient population that primarily undergo SCR. Thus, the biomechanical results of this controlled laboratory investigation may offer limited clinical utility in the in vivo setting.

Conclusion

The 4.5-mm Bio-Corkscrew anchor provided the most robust fixation to the glenoid during SCR as it demonstrated the highest maximum load, had minimal elongation, minimal first cycle excursion, and did not fail during cyclic testing. The superior glenoid neck had the highest BMD; however, there was no correlation between BMD or glenoid anchor location and biomechanical outcomes. The posterior portal and anterior portal provided optimal access to the posterosuperior glenoid neck and anterosuperior glenoid neck, respectively.

Disclaimers:

References

1. Agarwalla A, Puzzitiello RN, Leong NL, Shewman EF, Verma NN, Romeo AA, et al. A biomechanical comparison of two arthroscopic suture techniques in biceps tenodesis: whip-stitch vs. simple suture techniques. J Shoulder Elbow Surg 2019;28:1531-6. https://doi.org/10.1016/j.jse.2019.01.004.

2. Burkhart SS, Denard PJ, Adams CR, Brady PC, Hartzler RU. Arthroscopic superior capsular reconstruction for massive irreparable rotator cuff repair. Arthrosc Tech 2016;5:e1407-18. https://doi.org/10.1016/j.eats.2016.08.024.

3. Chahla J, Cancienne JM, Beletsky A, Manderle BJ, Verma NN. Arthroscopic superior capsular reconstruction with dermal Allograft for the treatment of a massive irreparable rotator cuff tear. JBJS Essent Surg Tech 2020;10:e19.00012. https://doi.org/10.2106/JBJS.ST.19.00012.

4. Chahla J, Liu JN, Manderle B, Beletsky A, Cabarcas B, Gowd AK, et al. Bony ingrowth of coil-type open-architecture anchors compared with screw-type PEEK anchors for the medial row in rotator cuff repair: a randomized controlled trial. Arthroscopy 2020;36:952-61. https://doi.org/10.1016/j.arthro.2019.11.119.

5. Cho C-H, Bae K-C, Kim D-H. Biomaterials used for suture anchors in orthopedic surgery. Clin Orthop Surg 2021;13:287. https://doi.org/10.4055/cios20317.

6. Denard PJ, Brady PC, Adams CR, Tokish JM, Burkhart SS. Preliminary results of arthroscopic superior capsule reconstruction with dermal Allograft. Arthroscopy 2018;34:93-9. https://doi.org/10.1016/j.arthro.2017.08.265.

7. Dwyer T, Willett TL, Dold AP, Petrera M, Wasserstein D, Whelan DB, et al. Maximum load to failure and tensile displacement of an all-suture glenoid anchor compared with a screw-in glenoid anchor. Knee Surg Sports Traumatol Arthrosc 2016;24:357-64. https://doi.org/10.1007/s00167-013-2760-0.

8. Goschka AM, Hafer JS, Reynolds KA, Aberle NS 2nd, Baldini TH, Hawkins MJ, et al. Biomechanical comparison of traditional anchors to all-suture anchors in a double-row rotator cuff repair cadaver model. Clin Biomech 2015;30:808-13. https://doi.org/10.1016/j.clinbiomech.2015.06.009.

9. Hirahara AM, Andersen WJ, Panero AJ. Superior capsular reconstruction: clinical outcomes after minimum 2-year follow-up. Am J Orthop (Belle Mead NJ) 2017;46:266-78.

10. Hyatt AEMD, Lavery KMD, Mino CBS, Dhawan AMD. Suture anchor biomechanics after rotator cuff footprint decortication. Arthroscopy 2015;32:544-50. https://doi.org/10.1016/j.arthro.2015.08.034.

11. Kerzner B, Swindell HW, Dasari SP, Khan ZA, Chahla J, Verma NN. Superior capsular reconstruction for irreparable rotator cuff tears: technique and associated considerations. Video J Sports Med 2022;2:263502542110731. https://doi.org/10.1177/26350254211073143.

12. Lin CL, Su FC, Chang CH, Hong YK, Jou IM, Lin CJ, et al. Effect of shoulder abduction on the fixation of humeral greater tuberosity fractures: a biomechanical study for three types of fixation constructs. J Shoulder Elbow Surg 2015;24:547-54. https://doi.org/10.1016/j.jse.2014.09.032.

13. Llanos-Rodríguez Á, Escandón-Almazán P, Espejo-Reina A, Nogales-Zafra J, Espejo-Baena A. Arthroscopic superior capsular reconstruction with Achilles tendon Allograft for massive and Revision rotator cuff tears. Arthrosc Tech 2022;11:e263-71. https://doi.org/10.1016/j.eats.2021.10.017.

14. Makovicka JL, Chung AS, Patel KA, Deckey DG, Hassebrock JD, Tokish JM. Superior capsule reconstruction for irreparable rotator cuff tears: a systematic review of biomechanical and clinical outcomes by graft type. J Shoulder Elbow Surg 2020;29:392-401. https://doi.org/10.1016/j.jse.2019.07.005.

15. Mazzocca AD, Chowaniec D, Cote MP, Fierra J, Apostolakos J, Nowak M, et al. Biomechanical evaluation of classic solid and novel all-soft suture anchors for glenoid labral repair. Arthroscopy 2012;28:642-8. https://doi.org/10.1016/j.arthro.2011.10.024.

16. Mihata T, Lee TQ, Watanabe C, Fukunishi K, Ohue M, Tsujimura T, et al. Clinical results of arthroscopic superior capsule reconstruction for irreparable rotator cuff tears. Arthroscopy 2013;29:459-70. https://doi.org/10.1016/j.arthro.2012.10.022.

17. Mihata T, McGarry MH, Pirolo JM, Kinoshita M, Lee TQ. Superior capsule reconstruction to restore superior stability in irreparable rotator cuff tears: a biomechanical cadaveric study. Am J Sports Med 2012;40:2248-55. https://doi.org/10.1177/0363546512456195.

18. Mimar R, Limb D, Hall RM. The relationship between glenoid bone density and the pullout strength of suture anchors. Shoulder Elbow 2009;1:31-4. https://doi.org/10.1111/j.1758-5740.2009.00003.x.

19. Ozturk BY, Ak S, Gultekin O, Baykus A, Kulduk A. Prospective, randomized evaluation of latissimus dorsi transfer and superior capsular reconstruction in massive, irreparable rotator cuff tears. J Shoulder Elbow Surg 2021;30:1561-71. https://doi.org/10.1016/j.jse.2021.01.036.

20. Pennington WT, Bartz BA, Pauli JM, Walker CE, Schmidt W. Arthroscopic superior capsular reconstruction with acellular dermal allograft for the treatment of massive irreparable rotator cuff tears: short-term clinical outcomes and the radiographic parameter of superior capsular distance. Arthroscopy 2018;34:1764-73. https://doi.org/10.1016/j.arthro.2018.01.009.

21. Pietschmann MF, Gülecyüz MF, Fieseler S, Hentschel M, Rossbach B, Jansson V, et al. Biomechanical stability of knotless suture anchors used in rotator cuff repair in healthy and osteopenic bone. Arthroscopy 2010;26:1035-44. https://doi.org/10.1016/j.arthro.2009.12.023.

22. Pogorzelski J, Muckenhirn KJ, Mitchell JJ, Katthagen JC, Schon JM, Dahl KD, et al. Biomechanical comparison of 3 glenoid-Side fixation techniques for superior capsular reconstruction. Am J Sports Med 2017;46:801-8. https://doi.org/10.1177/0363546517745626.

23. Poukalova M, Yakacki CM, Guldberg RE, Lin A, Saing M, Gillogly SD, et al. Pullout strength of suture anchors: effect of mechanical properties of trabecular bone. J Biomech 2010;43:1138-45. https://doi.org/10.1016/j.jbiomech.2009.12.007.

24. Salata MJ, Bailey JR, Bell R, Frank RM, McGill KC, Lin EC, et al. Effect of interference screw depth on fixation strength in biceps tenodesis. Arthroscopy 2014;30:11-5. https://doi.org/10.1016/j.arthro.2013.08.033.

25. Schon JM, Katthagen JC, Dupre CN, Mitchell JJ, Turnbull TL, Adams CR, et al. Quantitative and computed tomography anatomic analysis of glenoid fixation for superior capsule reconstruction: a cadaveric study. Arthroscopy 2017;33:1131-7. https://doi.org/10.1016/j.arthro.2016.10.016.

26. Slabaugh MA, Frank RM, Van Thiel GS, Bell RM, Wang VM, Trenhaile S, et al. Biceps tenodesis with Interference screw fixation: a biomechanical comparison of screw length and diameter. Arthroscopy 2011;27:161-6. https://doi.org/10.1016/j.arthro.2010.07.004.

27. Strauss E, Frank D, Kubiak E, Kummer F, Rokito A. The effect of the angle of suture anchor insertion on fixation failure at the tendon-suture interface after rotator cuff repair: deadman's angle revisited. Arthroscopy 2009;25:597-602. https://doi.org/10.1016/j.arthro.2008.12.021.

28. Tingart MJ, Apreleva M, Lehtinen J, Zurakowski D, Warner JJ. Anchor design and bone mineral density affect the pull-out strength of suture anchors in rotator cuff repair: which anchors are best to use in patients with low bone quality? Am J Sports Med 2004;32:1466-73. https://doi.org/10.1177/0363546503262644.

29. Tingart MJ, Apreleva M, Zurakowski D, Warner JJ. Pullout strength of suture anchors used in rotator cuff repair. J Bone Joint Surg Am 2003;85:2190-8. https://doi.org/10.2106/00004623-200311000-00021.

30. Tokish JM, Beicker C. Superior capsule reconstruction technique using an acellular dermal allograft. Arthrosc Tech 2015;4:e833-9. https://doi.org/10.1016/j.eats.2015.08.005.

31. Yamamoto N, Itoi E. Treatment of irreparable rotator cuff tears with superior capsular reconstruction. J Exp Orthop 2021;8:23. https://doi.org/10.1186/s40634-021-00342-1.